Clarification of Pathway-Specific Inhibition by Fourier Transform Ion Cyclotron Resonance/Mass Spectrometry-Based Metabolic Phenotyping Studies[1][W]

Akira Oikawa, Yukiko Nakamura, Tomonori Ogura, Atsuko Kimura, Hideyuki Suzuki, Nozomu Sakurai, Yoko Shinbo, Daisuke Shibata, Shigehiko Kanaya, and Daisaku Ohta*

Graduate School of Life and Environmental Sciences, Osaka Prefecture University, Sakai 599–8531, Japan (A.O., T.O., A.K., D.O.); Research Association for Biotechnology, Tokyo 105–0003, Japan (A.O., Y.S.); Department of Bioinformatics and Genomics, Nara Institute of Science and Technology, Ikoma 630–0192, Japan (Y.N., Y.S., S.K.); Ehime Women's College, Uwajima 798–0025, Japan (Y.N.); and Kazusa DNA Research Institute, Kisarazu 292–0818, Japan (Y.N., H.S., N.S., D.S.)

We have developed a metabolic profiling scheme based on direct-infusion Fourier transform ion cyclotron resonance mass spectrometry (FT-ICR/MS). The scheme consists of: (1) reproducible data collection under optimized FT-ICR/MS analytical conditions; (2) automatic mass-error correction and multivariate analyses for metabolome characterization using a newly developed metabolomics tool (DMASS software); (3) identification of marker metabolite candidates by searching a species-metabolite relationship database, KNApSAcK; and (4) structural analyses by an MS/MS method. The scheme was applied to metabolic phenotyping of Arabidopsis (*Arabidopsis thaliana*) seedlings treated with different herbicidal chemical classes for pathway-specific inhibitions. Arabidopsis extracts were directly infused into an electrospray ionization source on an FT-ICR/MS system. Acquired metabolomics data were comprised of mass-to-charge ratio values with ion intensity information subjected to principal component analysis, and metabolic phenotypes from the herbicide treatments were clearly differentiated from those of the herbicide-free treatment. From each herbicide treatment, candidate metabolites representing such metabolic phenotypes were found through the KNApSAcK database search. The database search and MS/MS analyses suggested dose-dependent accumulation patterns of specific metabolites including several flavonoid glycosides. The metabolic phenotyping scheme on the basis of FT-ICR/MS coupled with the DMASS program is discussed as a general tool for high throughput metabolic phenotyping studies.

Metabolomics constitutes one of the essential challenges in functional genomics studies, providing biochemical information for understanding complex metabolic activities of certain cells, tissues, organs, and individual organisms. Particularly, through comprehensive metabolomics, endogenous small molecules of unknown properties could be uncovered as to represent specific biological conditions, and chemical structure information for such molecules is crucial for a rational understanding of the occurrence of such unknown metabolites in a biological context. Thus, metabolite identification and structural characterization are essential for successful metabolomics.

Different analytical instruments have been applied to metabolome analyses (Fiehn, 2002; Sumner et al., 2003; Fernie et al., 2004), and specific advantages and disadvantages are associated with each of these analytical systems. Gas chromatography (GC) coupled with mass spectrometry (MS) is relatively low cost and easy to operate with a very long capillary column ensuring high separation efficiency for analyzing complex biological mixtures (Fiehn et al., 2000; Roessner et al., 2001; Kaplan et al., 2004). Compound libraries of ion fragmentation patterns can be also a great help for identification of metabolites of known properties. However, only volatile compounds could be detected by GC-MS, and samples must be derivatized before analysis. Moreover, GC-MS is not applicable to the analyses of heat-labile compounds, and molecular identification of unknown metabolites also undergoes difficulties with GC-MS analyses. Liquid chromatography (LC) coupled with MS is a prevalent system in metabolomics studies (Huhman and Sumner, 2002; Wu et al., 2005). Combinations of various columns, solvents, and ionization methods can be applied for LC-MS, covering a wide range of compounds of different properties. However, separation/analytical conditions should be adjusted for different chemical classes. Capillary electrophoresis (CE) coupled with MS is a highly selective and efficient system for polar compounds such as amino acids, sugars, and nucleic acids (Soga et al., 2003; von Roepenack-Lahaye et al., 2004). The CE-MS system is not suitable for

[1] This work was supported by the New Energy and Industrial Technology Development Organization, Japan, and in part by the Ministry of Education, Culture, Sports, Science, and Technology of Japan (grant no. 16580281 to D.O.).

* Corresponding author; e-mail ohtad@bioinfo.osakafu-u.ac.jp; fax 81–72–254–9409.

The author responsible for distribution of materials integral to the findings presented in this article in accordance with the policy described in the Instructions for Authors (www.plantphysiol.org) is: Daisaku Ohta (ohtad@bioinfo.osakafu-u.ac.jp).

[W] The online version of this article contains Web-only data.

www.plantphysiol.org/cgi/doi/10.1104/pp.106.080317

nonpolar metabolites in biological samples. The time-consuming separation processes (GC, LC, and CE) prior to the MS analyses could not be advantageous for developing a high-throughput metabolomics system. Besides these hyphenated methods, NMR has been introduced for metabolomics research to aid in the applicability for rapid and simultaneous analyses of complex biological samples (Aranìbar et al., 2001; Viant et al., 2003; Choi et al., 2004). However, NMR-based metabolomics could be disadvantageous due to its relatively low sensitivity. Other difficulties may also arise from the molecular identification of each metabolite in complex samples from chemical shift assignment.

Fourier transform ion cyclotron resonance MS (FT-ICR/MS) offers high-throughput analyses of small molecules at extremely high levels of resolution and sensitivity, typically being under four or five places of decimals in the mass measurements. Such accurate FT-ICR/MS analyses can be applied to the prediction of chemical formulas and molecular identities of metabolites. The direct infusion analyses using FT-ICR/MS technology is thus the best-suited option for high-throughput metabolic profiling studies coupled with a metabolite identification scheme. However, FT-ICR/MS has been mainly applied to proteomics research, and its extreme performance has not been fully developed as a general metabolomics tool.

Here, we describe a metabolomics research scheme with a computational tool, DMASS, developed exclusively for metabolic profiling studies using FT-ICR/MS.

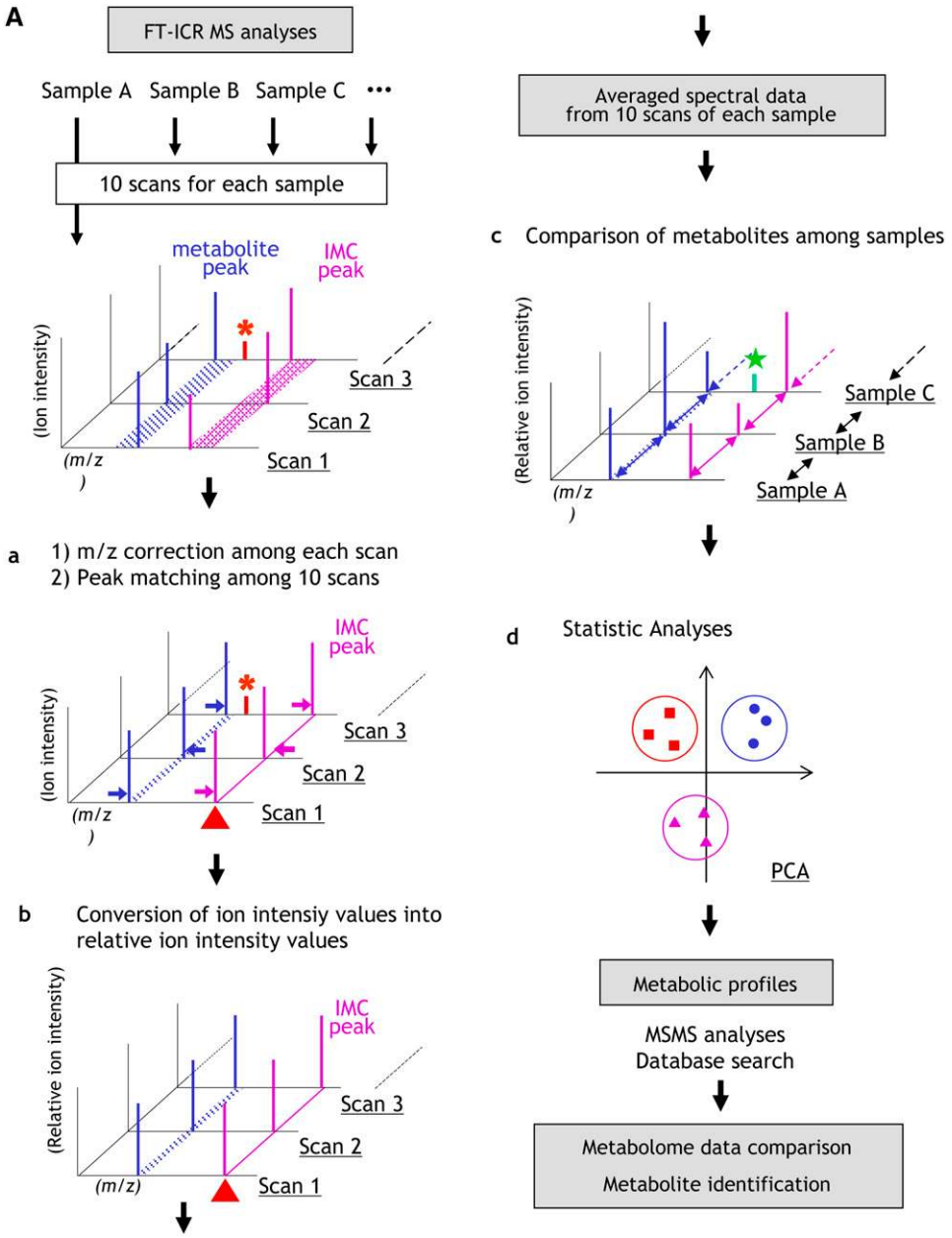

Figure 1. A, Schematic view of the DMASS data processing. Ten mass spectral data were successively acquired from each sample and processed by the following steps. The shadowed ribbons (blue and magenta) indicate the *m/z* fluctuations. a, The experimental *m/z* values of the IMCs were fixed to their theoretical *m/z* values (the red triangle), and the *m/z* calibration data were used for the *m/z* value correction for all other ion species in each spectral scan. Then, the corrected *m/z* values (ion peaks) of 10 independent scans were identified to one another (peak matching). Irreproducible ions (such as the peak indicated by the asterisk) were excluded from further data processing. Arrows indicate schematically the *m/z* value correction step. b, Ion intensity values of reproducibly observed ions from each spectral scan were converted into percentage values of total ion intensity (relative ion intensity values). c, Metabolome data of a single biological sample consisted of the averaged spectral data (*m/z* values and ion intensity values) from 10 scans. Specific ions from individual samples (as those indicated by the star) were included for the metabolome comparison by multivariate analyses. Arrows indicate schematically the peak matching among samples. d, Metabolome data were subjected to multivariate analyses reflecting biological conditions. B, Operation window of DMASS. Lowercase letters (a–d) indicate each step of the DMASS scheme described above.

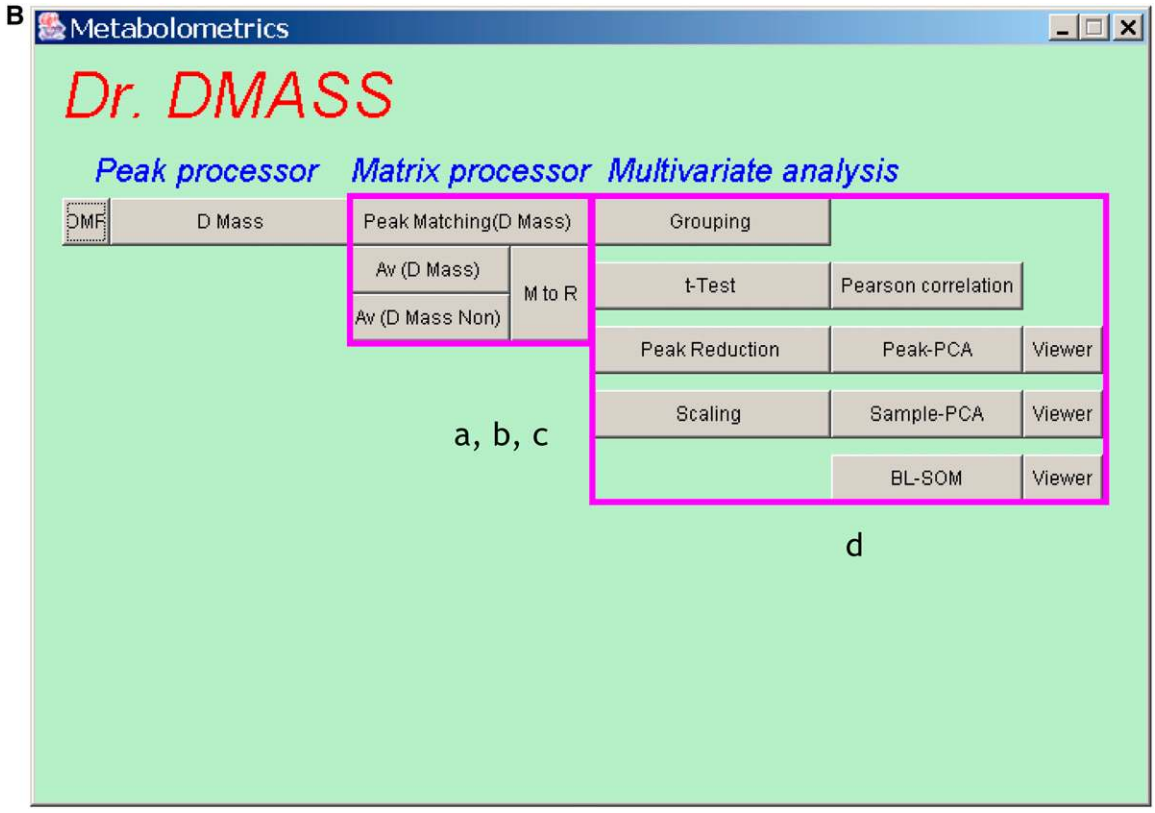

Figure 1. (*Continued.*)

The DMASS scheme converts thousands of mass signals (mass-to-charge ratio [*m/z*] values and ion intensity values) into metabolome data through several steps, including correction of *m/z* values using internal mass calibrants (IMCs), averaging ion intensities of individual MS signals among replicate samples, and multivariate analyses such as principal component analysis (PCA) and batch learning-self organizing map. We studied how our FT-ICR/MS with the DMASS data processing scheme is functional for metabolic profiling and phenotyping studies. We mimicked specific metabolic disorders by treating Arabidopsis (*Arabidopsis thaliana*) seedlings with herbicides of known mode of actions. The DMASS scheme and the PCA revealed distinct metabolome clusters among those herbicide treatments, and detailed comparison of the metabolomes led to identification of specific metabolite accumulation in each herbicide treatment. Using a metabolite-species database (KNApSAcK, http://kanaya.naist.jp/KNApSAcK/), we succeeded in predicting metabolite identification, and these structures were further investigated in the MS/MS analyses using a sustained off resonance irradiation-collision induced dissociation (SORI-CID) method of the FT-ICR/MS. These results demonstrated practical application possibilities of the FT-ICR/MS-based metabolic phenotyping as an essential function in integrated metabolomics studies.

RESULTS AND DISCUSSION

FT-ICR/MS Data Processing System

One of the major objectives in our metabolomics studies was metabolite identification with the aid of high-resolution mass spectral data and ion signal intensity information, leading to characterization of metabolic profiles representing biological conditions. For such metabolite identification, FT-ICR/MS is the best technology owing to its extreme levels of accurate mass determination and high-resolution performance. However, at least in our system, analytical data fluctuations were generally associated with the *m/z* values at the levels of three or four places of decimals in the high-resolution analyses with FT-ICR/MS. In addition, the ion signal intensities fluctuated in every spectral scanning. Without managing such analytical difficulties, FT-ICR/MS could not be applied to reproducible metabolomics studies. We developed a data analysis tool, DMASS, for large-scale metabolic profiling studies on the basis of FT-ICR/MS analyses. Figure 1 shows schematically the data processing steps.

For FT-ICR/MS measurements, we performed 10 successive spectral scans for each sample analysis. For the analysis, we added IMCs to experimental samples for correcting the analytical errors with *m/z* values. These IMCs included lidocaine, prochloraz, reserpine, and bombesin for the positive ion mode analysis, and

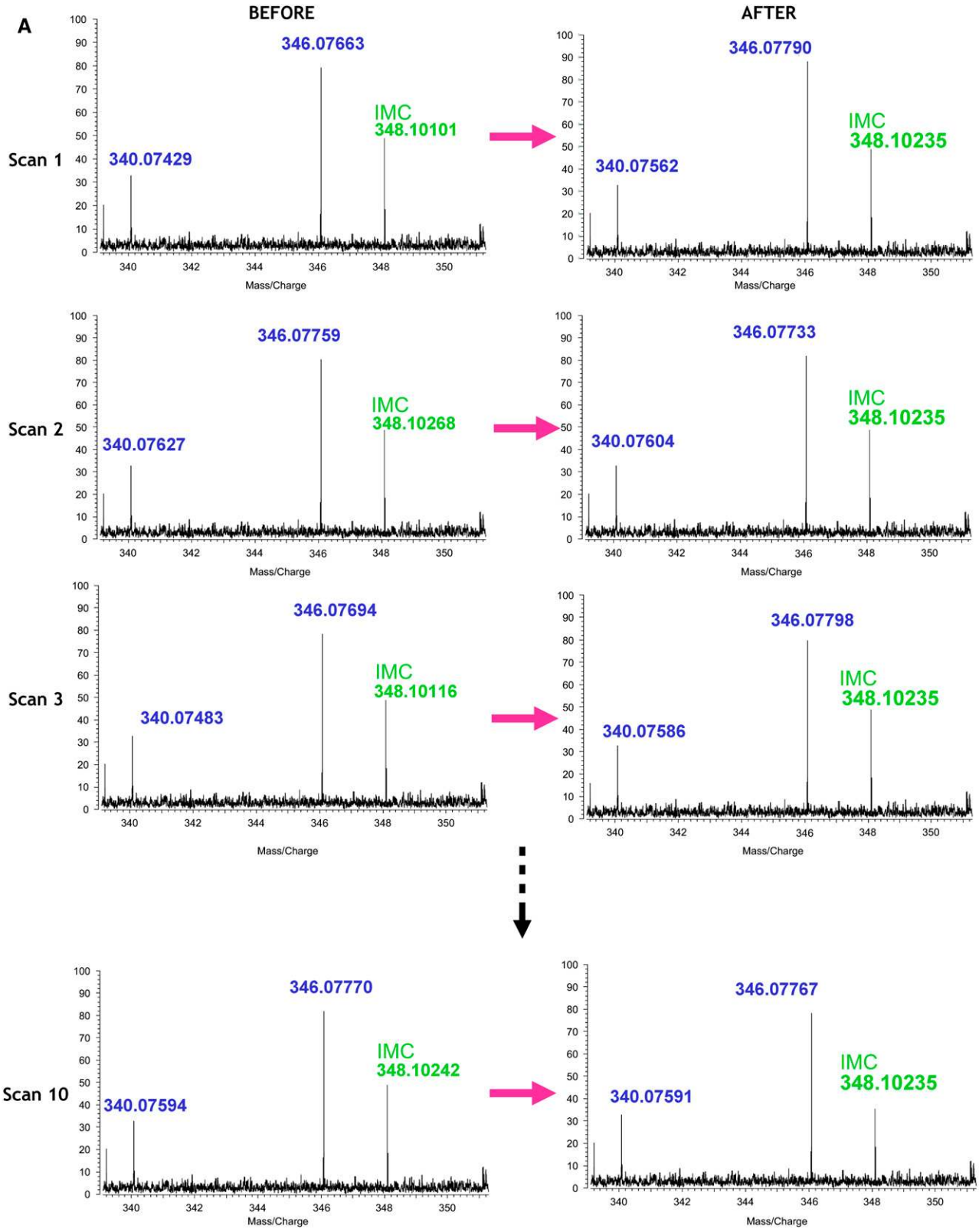

Figure 2. A, An actual example of the correction of *m/z* values. A raw mass spectral data set (*m/z* values) from 10 scans (before) was corrected by the DMASS scheme (after). The ion signals derived from ampicillin, added as an IMC, are shown in green. The *m/z* values of ampicillin were fixed to its theoretical *m/z* value (348.10235). The experimental *m/z* values of other IMCs were also fixed. Then, the *m/z* errors found with the IMCs were reflected for the compensation of *m/z* values of other ions. B, CV of the *m/z*

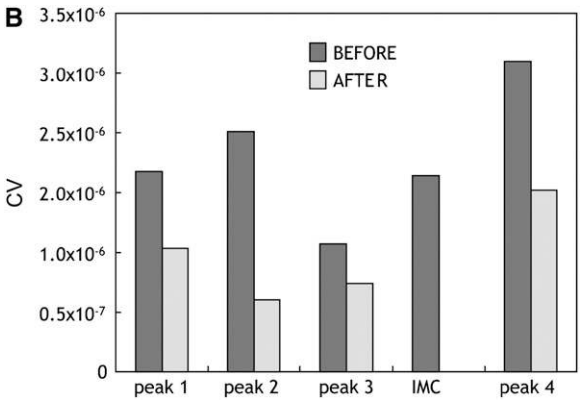

Figure 2. (*Continued.*)

a set of 2,4-dichlorophenoxy acetic acid, ampicillin, 3-[(3-cholamidopropyl) dimethylammonio]propanesulfonic acid, and tetra-*N*-acetylchitotetraose was used as the IMCs for the negative ion mode analysis. Briefly, the experimental *m/z* values of the IMCs were fixed to their theoretical values, and the *m/z* error calibration data were reflected for the *m/z* compensation for all other ion species in each spectral scan (Figure 1A, a). Then the corrected *m/z* values of repeatedly identifiable *m/z* values were matched to one another among 10 independent scans (Fig. 1A, b). Ions (*m/z* values) such as those shown by the asterisk in Figure 1A, a, in which appearance frequencies were below 50% among 10 independent scans, for example, were not included for further data processing steps. The threshold levels of ion appearance frequencies were freely adjustable in the DMASS data processing scheme. The intensity values of reproducibly observed ions were converted into percentage values of total ion intensity (Fig. 1A, b). Thus, metabolome data from a single biological sample consisted of averaged *m/z* values with intensity information from 10 spectral scans. These data processing steps were applied to metabolome comparison among different samples (Fig. 1A, c) using multivariate analyses reflecting biological conditions (Fig. 1A, d). Specific ions observed with individual samples, such as the ion indicated by the star in Figure 1A, c, were included for the multivariate analyses. Figure 1B shows the DMASS operation window for the automatic analytical steps (Fig. 1A, a–d).

Figure 2A shows an actual example of the *m/z* value fluctuations from a plant extract analysis in the negative ion mode. The peak of $m/z = 348.10101$ in scan 1, corresponding to ampicillin added as an IMC, was seen with the *m/z* values of 348.10268 and 348.10116 in scan 2 and scan 3, respectively. In every spectral scanning, such fluctuations of experimental *m/z* values were also detected with other ion peaks at a level corresponding to molecular weight (MW) < 0.002. We corrected the analytical errors with the IMCs in 10 independent spectral scans for a single sample. For example, the experimental *m/z* values of ampicillin in spectral scan (scan 1 through scan 10) were fixed to its theoretical value of 348.10235 (Fig. 2A, after). The *m/z* values of the other IMCs were fixed as well, and analytical errors with all other *m/z* values were compensated in terms of the corrected *m/z* values with the IMCs. Figure 2A schematically shows that the *m/z* values of 340.07429 and 346.07663 in scan 1 (before) were automatically converted to 340.07562 and 346.07790 (after), respectively, by DMASS software. The analytical errors in every spectral scanning were similarly compensated (Fig. 2A). Through this *m/z* compensation step, fluctuations of *m/z* values were narrowed down to a deviation range smaller than MW = 0.001. Significant numbers of ion species were not reproducibly detected among 10 independent scans from a single sample. The signal intensities of such ions with low appearance frequencies were notably low compared with repeatedly observed ions and were excluded from further data processing steps. Reproducible ions should have included both common ions among different samples and unique ions present in each specific sample. We studied whether the DMASS scheme satisfactorily corrected the *m/z* fluctuations. Thus, we compared the *m/z* fluctuations in terms of the coefficient of variance (CV), which was obtained by dividing the SD value for each *m/z* fluctuation by its averaged *m/z* value. Figure 2B shows an example of a CV value comparison before and after the DMASS data processing. After the analytical error correction, the *m/z* fluctuation for each ion decreased in the entire range of MW of our interest (data not shown).

The signal intensities of the reproducibly detectable ions were compared among 10 independent scans of each sample using the DMASS scheme. After compensating for the *m/z* value fluctuations, we were able to match corresponding ions to one another among different spectral scans. Between independent spectral scans of different extracts from a single sample, the intensity values of 95% of ion species were within 1.46-fold deviation, 90% were within 1.34-fold deviation, 75% within 1.19-fold, 50% within 1.10-fold, and 25% of ion species were within 1.04-fold deviation (Fig. 3A). Figure 3B shows the ion intensity fluctuations between two independent Arabidopsis samples from a standard growth condition. The intensity values of 95% of ion species were within 2.40-fold deviation, 90% were

Figure 2. (*Continued.*)
values among 10 spectral scans were compared before and after the DMASS data processing: peak 1 ($m/z = 339.20060$), peak 2 ($m/z = 340.07588$), peak 3 ($m/z = 346.07773$), peak 4 ($m/z = 351.11997$), and IMC (ampicillin). The CV values were obtained by dividing the SD value for each *m/z* fluctuation by the averaged *m/z* value.

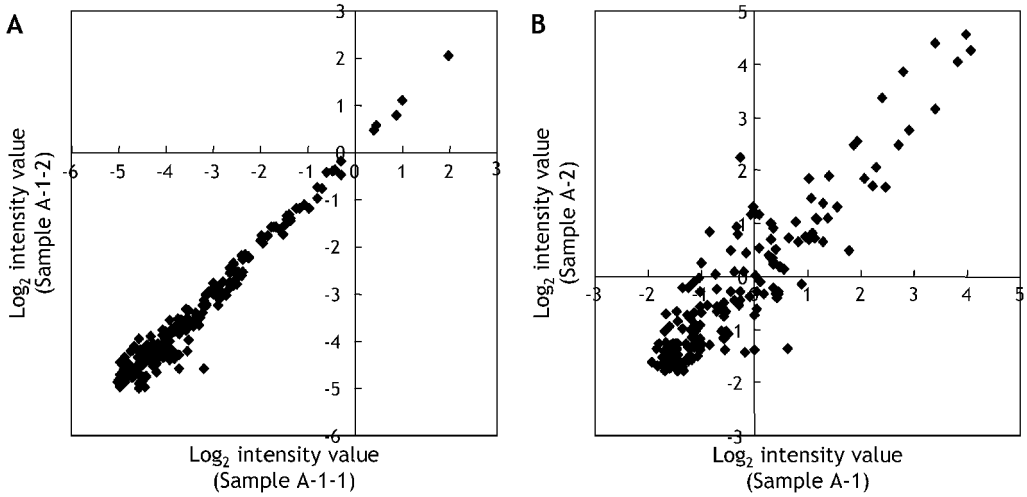

Figure 3. Reproducibility of ion intensity values. A, Ion intensity values were compared between two independent extracts from a single sample. B, Ion intensity fluctuations were compared between two independent Arabidopsis samples from a standard growth condition.

within 1.93-fold deviation, 75% within 1.50-fold, 50% within 1.24-fold, and 25% were within 1.10-fold deviation. These ion intensity fluctuations were comparable to those observed with a different FT-ICR/MS system (Aharoni et al., 2002). Taken together, the analyses of the same sample were less influenced by different extraction processes (Fig. 3A), while the metabolomes even from the same growth conditions might have fluctuated due to biological reasons (Fig. 3B). In the mass ranges of 55 to 400 and 400 to 1,000 of our FT-ICR/MS analyses, the averages of analytical errors (calculated from absolute *m/z* values) were 0.000282 and 0.000703, respectively, and the corresponding SDs were 0.000361 and 0.000923, respectively.

As described above, our metabolic profiling data from each sample consisted of corrected *m/z* values with averaged signal intensity values of reproducible ions from 10 independent spectral data. We prepared at least triplicate samples for each experimental treatment, and the corresponding ions were identified and matched one to another among triplicate samples. In addition to these data processing steps, we performed statistical analyses of *t* test and Pearson correlation coefficient for individual ions (Fig. 1B, d). Metabolome comparison among different samples was done using two multivariate analyses, PCA and batch learning-self organizing map (Fig. 1B, d), which are extensively used as bioinformatics tools for clarification of metabolomes according to metabolite accumulation profiles (Kanaya et al., 2001; Abe et al., 2003; Hirai et al., 2004, 2005). The software, Dr.DMASS, is downloadable with detailed instructions at the Web site (http://kanaya.aist-nara.ac.jp/DrDMASS/).

Metabolic Profiling

The entire scheme of the DMASS data processing was applied to the profiling of metabolic disorders caused by a variety of chemicals with different herbicidal modes of action. Arabidopsis seedlings were treated at concentrations of herbicides shown in Table I, and methanol extracts were directly applied to the metabolic profiling analyses. Figure 4 shows the growth inhibition curves of Arabidopsis seedlings treated with herbicides (Table I). As the inhibitors for acetolactate synthase (ALS), we used sulfonylureas (halosulfuron and pyrazosulfuron) and an imidazolinone (imazamox), and two different chemical classes of cyclohexanediones (CHDs; clethodim and alloxidim) and aryloxyphenoxypropionates (AOPPs; quizalofop and cyhalofop) were used as the inhibitors of acetyl-CoA carboxylase (ACCase). The herbicides used in this study, except for cyhalofop, strongly inhibited Arabidopsis growth in dose-dependent manners. When treated with cyhalofop even at higher concentrations, no significant growth inhibition was observed. In the growth inhibition test, ALS inhibitors were 100 to 1,000 times more potent than other herbicides. For the metabolic profiling studies, we set the IC50 values (the concentration required for 50% growth inhibition) as the highest concentrations for the herbicide treatment to be analyzed by our metabolic profiling scheme (Fig. 4).

We set the analytical conditions for reproducible detection of 200 to approximately 300 independent ions from each sample, while extreme conditions could be applied to observe thousands of ions from each scanning. Nonetheless, a total of 1,560 independent ions in the positive and the negative ion mode analyses were detected from the different herbicide treatments (Supplemental Data S1). These results indicated that different ion species were detected from each of these herbicide treatments, suggesting that unique sets of metabolites built up in the different herbicide treatments. In other words, our FT-ICR/MS analytical condition for simultaneous detection of

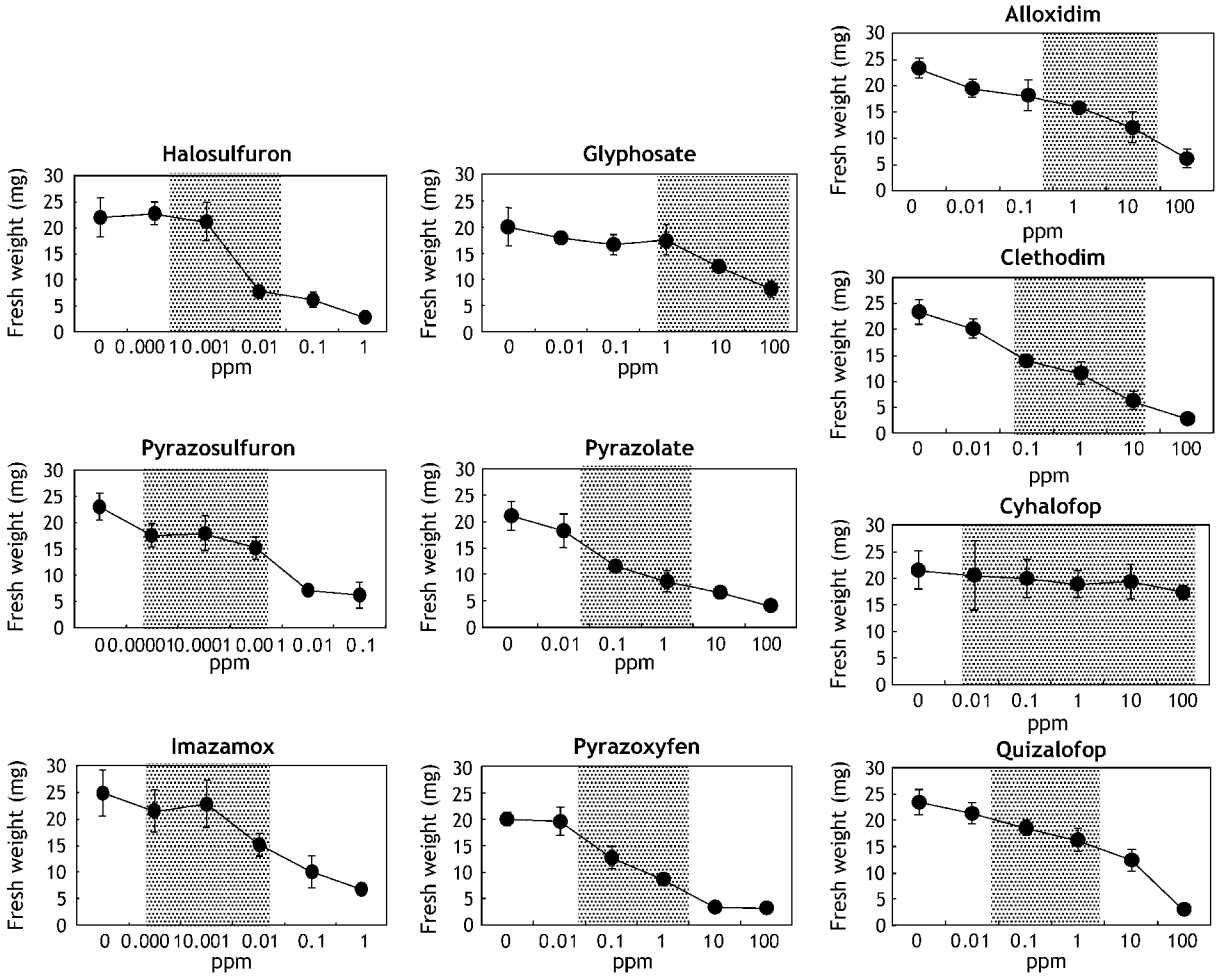

Figure 4. Growth inhibition of Arabidopsis seedlings treated with different herbicides. Plant growth was recorded after a 7-d treatment with herbicides. The concentration ranges of herbicides used in metabolic profiling studies were shaded. Error bars indicate SDs of three replicates.

about 200 to approximately 300 ions was sufficient for metabolic profiling in this experimental design, while it is postulated that Arabidopsis may produce more than 5,000 compounds (Roessner et al., 2001). Newly appeared ion species were as high as 534 in these herbicide treatments, and the intensity values of 518 ions out of the 1,560 ion species have increased or decreased by over 2-fold from the differential herbicide treatments. We identified metabolite candidates for 284 ions (Supplemental Data S1) by searching the species-metabolite relationship database KNApSAcK, containing 11,075 metabolites (at the end of January, 2006), mainly from plant taxa (Shinbo et al., 2006).

In the direct infusion electrospray ionization (ESI) FT-ICR/MS analyses, thousands of ions could be detected from each spectral scan by increasing the ion accumulation time at the hexapole. However, those ions were not reproducibly detected. The ions accumulated in excess could not transfer into the FT-ICR cell, and the amounts of ions in the cell could not be maintained persistently during successive spectral scanning (data not shown). Unexpected collisions among excess ions could also occur in the analyzing cell generating unnatural ions. The same difficulties should also arise at the hexapole region accumulating excess amounts of ions. In addition, we found that extended accumulation time at the hexapole led to the generation of multiply charged ions from a single ion species (data not shown). In this study, the FT-ICR/MS analytical condition for detecting 200 to approximately 300 ion species was satisfactorily applied to metabolic profiling studies without suffering from unnecessary difficulties due to irreproducible ions among spectral scans.

PCA for Metabolic Phenotyping

Figure 5 shows the metabolome clusters demonstrated by PCA using DMASS software. PCA is a multivariate regression method to project a distribution of data points in a multidimensional space into a space of fewer dimensions. In Figure 5, two vectors of

Table I. *Herbicides used in the experiments*

Treatment (Abbreviation)	Mode of Action	Chemistry	IC50[a]	Reference[b]
			μM	
Glyphosate (Glp)	EPSPS inhibitor	*N*-phosphono-glycine	10 to approximately 400	5, 6
Halosulfuron (Has)	ALS inhibitor	Sulfonylurea	18 to approximately 140[c]	12
Pyrazosulfuron (Pys)	ALS inhibitor	Sulfonylurea	0.42 to approximately 12.87	1
Imazamox (Imz)	ALS inhibitor	Imidazolinone	35 to approximately 45[c]	12
Pyrazoxyfen (Pyz)	4HPPD inhibitor	Pyrazole	3,000[c]	12
Pyrazolate (Pyl)	4HPPD inhibitor	Pyrazole	2,000 to approximately 3,000[c]	12
Alloxydim (Ald)	ACCase inhibitor	Cyclohexenone	2.0 to approximately 9.6	8
Clethodim (Cld)	ACCase inhibitor	Cyclohexenone	0.15	8, 9, 11
Quizalofop (Quf)	ACCase inhibitor	4AOPP	0.03 to approximately 57	2, 3, 4, 10
Cyhalofop (Cyf)	ACCase inhibitor	4AOPP	8.91	7

[a]Concentration for 50% inhibition of enzyme activities. [b]Cited references. Reference are as follows: (1) Kuk et al. (2003), (2) Dehaye et al. (1994), (3) Konishi and Sasaki (1994), (4) Herbert et al. (1996), (5) Widholm et al. (2001), (6) Huynh et al. (1988), (7) Ruiz-Santaella et al. (2006), (8) Lichtenthaler (1990), (9) Délye et al. (2003), (10) Price et al. (2003), (11) Délye et al. (2005), and (12) Hirai et al. (2002). [c]Application rate (active ingredient g ha^{-1}).

principal component 1 (PC1 = 30.7%) and principal component 2 (PC2 = 15.6%) were sufficient to distinguish the metabolic disorders caused by the specific enzyme inhibitions. The metabolome cluster from the lower concentrations of herbicide treatments was not separated from that of the control samples (herbicide-free metabolome; circled with black solid line). When treated with higher concentrations of herbicides, metabolomes were classified into four distinct clusters: 5-enolpyruvylshikimate-3-P synthase (EPSPS) inhibition (blue), ALS inhibition (red), 4-hydroxyphenylpyruvate dehydrogenase (4HPPD) inhibition (purple), and ACCase inhibition (green). The metabolome observed with the ALS inhibitor treatments formed a single cluster irrespective of the inhibitor classes of sulfonylureas and an imidazolinone. This was also the

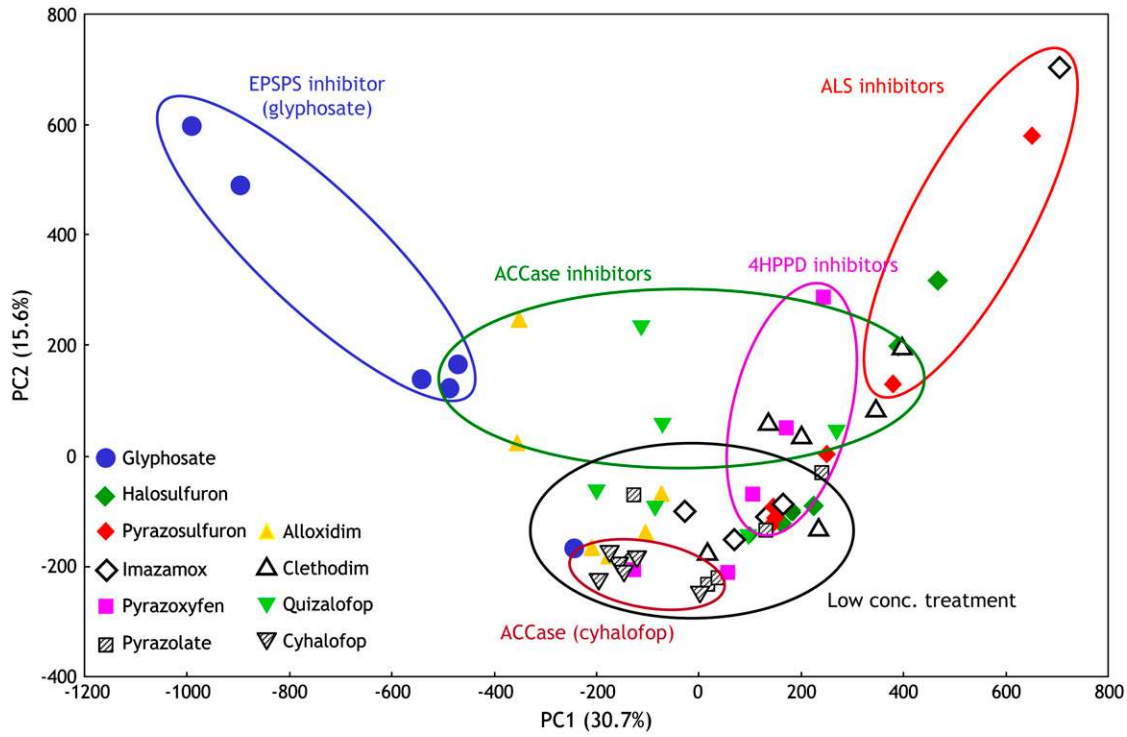

Figure 5. Metabolome clusters demonstrated by PCA. PC1 and 2 with the contribution ratios of 30.7% and 15.6%, respectively, were sufficient to differentiate the metabolic disorders caused by the herbicide treatments. The metabolome cluster from the lower concentrations of herbicide treatments was circled in black. Treatment with higher concentrations of herbicides gave four distinct metabolome clusters: EPSPS inhibition (blue), ALS inhibition (red), 4HPPD inhibition (purple), and ACCase inhibition (green). The metabolomes observed with the cyhalofop treatments were not separated from those of the control samples (brown).

case for the ACCase inhibition by two different chemical classes of the CHDs and the AOPP. These results suggested that we detected the metabolic disorders caused by the inhibition of the specific enzymatic steps, but they were not due to unidentified side effects by the herbicide treatments. The metabolome from the cyhalofop treatment, which had no growth inhibition effects on Arabidopsis, was indistinguishable from that of the control experiments (brown circle in Fig. 5). Ions corresponding to herbicides were not detected under our experimental conditions. This was probably due to the fact that extremely low concentrations of herbicides were sufficient for the growth inhibition (Fig. 4).

Our metabolomics studies were directed to determine differential metabolic profiles using the direct infusion ESI/FT-ICR/MS, where ion suppression effects were unavoidable. Ion suppression is a phenomenon in which compounds present in a complex mixture at high concentrations compete against other compounds at the ionization step, and these compounds can affect the ion intensity values of individual compounds in sample solutions. In other words, differential ion suppression effects should occur for every metabolite in different samples, and the ion intensity values for such metabolites could not be easily compared among different samples. We designed our experiments to detect dose-dependent metabolic disorders caused by the herbicide treatments. Thus, we were able to ascribe differential metabolic profiles to such herbicide treatments (inhibition of specific enzymatic steps) monitoring dose-dependent metabolite

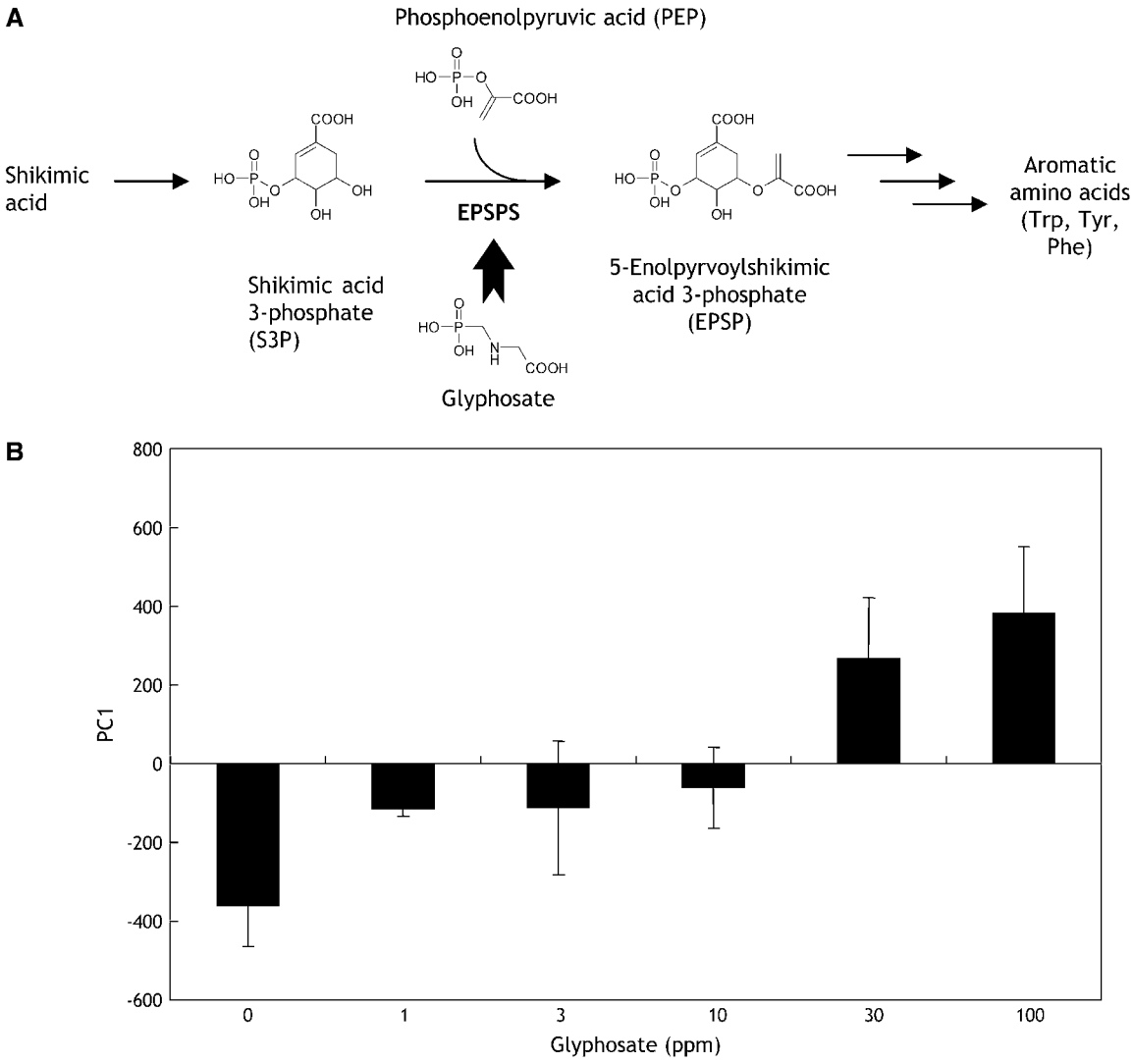

Figure 6. A, A part of shikimic acid pathway. Glyphosate inhibits the EPSPS reaction yielding 5-enolpyrvoylshikimic acid 3-P from S3P and phospho*enol*pyruvate. B, PC1 values were obtained from the glyphosate treatments of different concentrations. A dose-dependent metabolic disorder caused by the glyphosate treatments was demonstrated by PC1 with the contribution ratio of 78.3%.

fluctuation patterns (changes in the ion intensity values). This metabolic profiling scheme could be applied to time-course experiments as well, while simple comparison between single dose treatments from a fixed time point would not be a reliable choice under the ion suppression effects.

Glyphosate Treatment Metabolome

Glyphosate inhibits EPSPS, which converts shikimic acid 3-P (S3P) with phospho*enol*pyruvate to 5-enolpyrvoylshikimic acid 3-P in the shikimic pathway (Steinrücken and Amrhein, 1980), producing the aromatic amino acids (Fig. 6A). The PCA for the glyphosate treatment demonstrated the formation of metabolomes in a dose-dependent manner, which was clarified on the PC1 with the contribution ratio of 78.3% (Fig. 6B). In the PCA, we were able to identify the components (metabolites) influencing such metabolome cluster formation. In the glyphosate treatment, an ion with m/z = 253.01115 in the negative ion mode analysis was revealed to have affected the metabolome cluster formation. The intensity of this ion increased in a dose-dependent manner (Fig. 7A), and the accumulation of this ion was specific for the glyphosate treatment (Fig. 7B). The KNApSAcK database search suggested S3P [theoretical m/z = 253.01188 ($[M-H]^-$), Δ m/z = 0.00073], which is the substrate of EPSPS, for this ion. We investigated the chemical structure of this metabolite by the MS/MS analysis using the SORI-CID technique. SORI utilizes off-resonance excitation of the ion under investigation (Gauthier et al., 1991), and SORI-CID is easy to implement as a collision activation technique and has been widely applied in FT-ICR/MS experiments (Laskin and Futrell, 2005). In the MS/MS spectrum, two fragment ions (m/z = 96.97130 and 235.00191) in addition to a target ion (m/z = 253.01115) were observed (Fig. 7C). The ion with m/z = 96.97130 could be assigned as phosphoric acid ($H_2PO_4^-$; theoretical m/z = 96.96962), and m/z = 235.00191 was

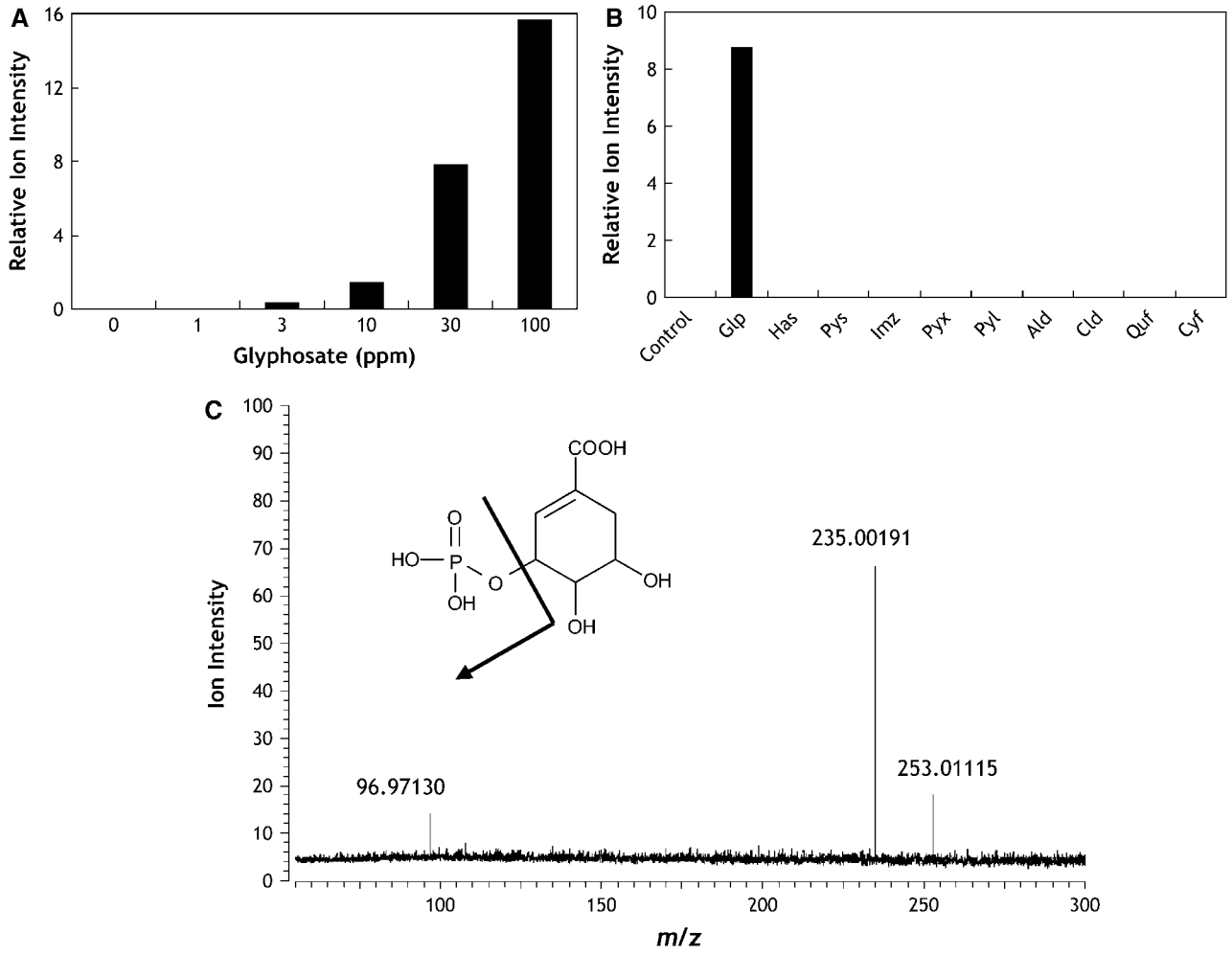

Figure 7. A, Dose-dependent accumulation of an ion with m/z = 253.01115 in the glyphosate-treated Arabidopsis seedlings. B, Accumulation of an ion with m/z = 253.01115 in Arabidopsis seedlings treated with herbicides. Abbreviations for herbicides used for the metabolome analyses were shown in Table I. C, MS/MS spectrum for an ion with m/z = 253.01115.

ascribed to dehydrated S3P (theoretical *m/z* = 235.00132), indicating strongly that the ion accumulated in the glyphosate-treated plants was in fact S3P. To our knowledge, this is the first case of the isolation of S3P from plant tissues. In the other herbicide treatments, accumulations of the enzyme substrates (pyruvate or 2-keto-lactate for ALS, 4-hydroxyphenylpyruvate for 4HPPD, and acetyl-CoA for ACCase) were not observed. This was probably due to the fact that these metabolites served as substrates for a wide range of biochemical reactions, and the lifetime of these metabolites in the plant cell should be quite short.

ACCase Inhibition Metabolome

Arabidopsis growth was strongly inhibited when treated with the ACCase inhibitors of quizalofop, alloxidim, and clethodim at the concentrations of 0.1 to approximately 1 ppm, while no growth inhibition was evident in the cyhalofop treatment (Fig. 4). The PCA (Fig. 5) demonstrated that the ACCase

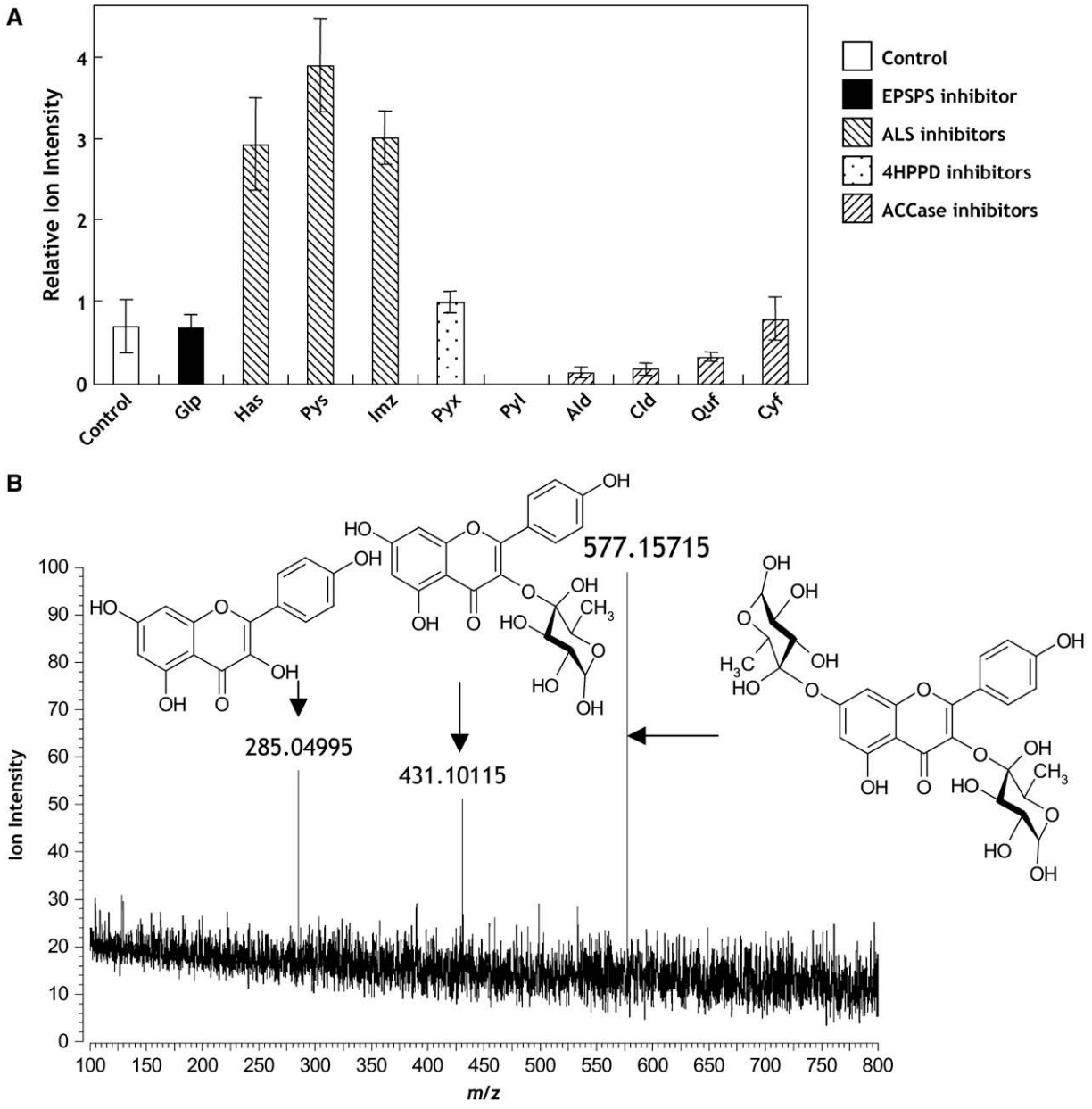

Figure 8. A, An ion (*m/z* = 577.15715) accumulated in Arabidopsis seedlings. Abbreviations for herbicides used for the metabolome analyses were shown in Table I. Error bars indicate SDs of three replicates. B, MS/MS fragmentation spectrum from the parent ion with *m/z* = 577.15715. Possible compound structures predicted by the KNApSAcK database search were indicated.

inhibition metabolome was clearly different from the herbicide-free metabolome (Fig. 5), and the metabolome of the cyhalofop-treated plants was in the cluster of the herbicide-free treatment.

The inhibition of ACCase activity with two different chemical classes, CHDs and AOPPs, is a well-established herbicidal mode of action. Most non-Poaceae species are insensitive to the ACCase inhibitors, and CHDs and AOPPs therefore constitute effective graminicide herbicides (Konishi and Sasaki, 1994; Délye et al., 2003). Only the multifunctional chloroplastic ACCase form, which is sensitive to these inhibitor classes, is functional in Poaceae plants, thereby being susceptible to those herbicides. Dicotyledonous plants contain two ACCase forms: a cytosolic multifunctional enzyme that is less sensitive to ACCase inhibitors compared with the chloroplastic multifunctional enzyme, and a plastidial multisubunit-type enzyme that is insensitive to the inhibitors (Konishi and Sasaki, 1994). In this study, we used CHD-type herbicides (alloxidim and clethodim) and AOPP-type herbicides (quizalofop and cyhalofop).

Both the AOPP (quizalofop) and the CHDs (alloxidim and clethodim) exhibited herbicidal effects on Arabidopsis, and this is a rather unexpected result from the well-known sensitivities of the ACCase forms. However, the metabolome analyses together with specific metabolite accumulations indicated that these herbicides actually impaired metabolic conditions, leading to the strong growth inhibition. It has been reported that specific residues in the carboxyltransferase domain were involved in the herbicide

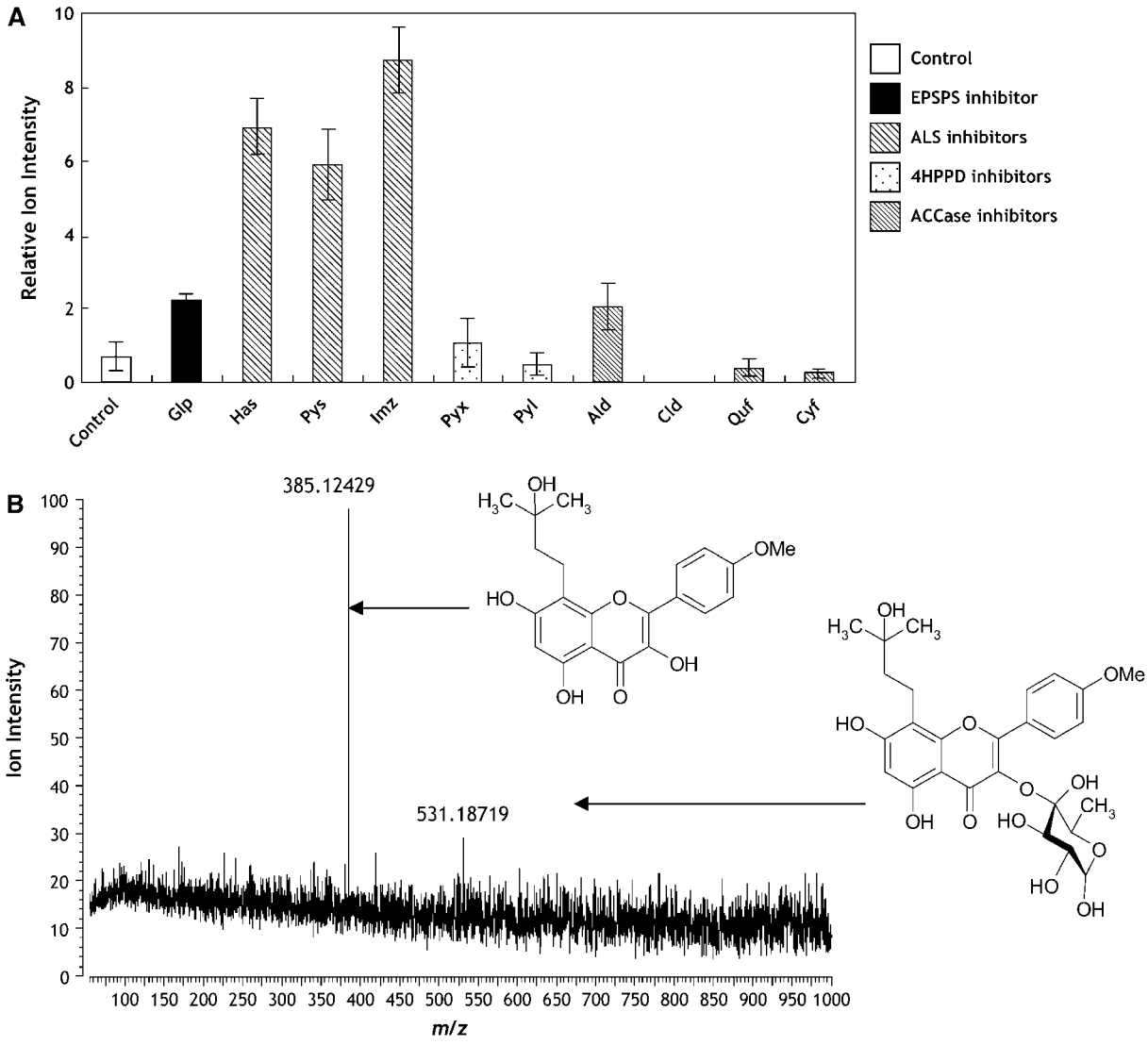

Figure 9. A, An ion (m/z = 531.18719) accumulated in Arabidopsis seedlings. Abbreviations for herbicides used for the metabolome analyses were shown in Table I. Error bars indicate SDs of three replicates. B, MS/MS fragmentation spectrum from the parent ion with m/z = 531.18719. Possible compound structures for these ions predicted by the KNApSAcK database search were indicated.

sensitivity (Moss et al., 2003). In the chloroplastic ACCase from *Alopecurus myosuroides* (black grass), the Ile-1781-Leu substitution conferred resistance to AOPPs and CHDs (Délye et al., 2003). In addition, the Ile-2041-Asn substitution was suggested to be involved in the resistance to AOPPs but not to CHDs. Protein crystallography using the yeast (*Saccharomyces cerevisiae*) multifunctional ACCase protein demonstrated that these amino acid residues were located in the binding site of the inhibitors (Zhang et al., 2004). In Arabidopsis, *ACC1* (At1g36160) and *ACC2* (At1g36180) genes encode the multifunctional enzymes. ACC1 has been reported to be located in cytosol, and ACC2 could be a plastidic form with an N-terminal extension of transit peptide properties (Baud et al., 2003). In these Arabidopsis enzymes, the corresponding sites were conserved as Leu (at the positions of 1759 and 1819) and Ile (at the positions of 1974 and 2079) residues in ACC1 and ACC2 proteins, respectively (Délye et al., 2003, 2005). These

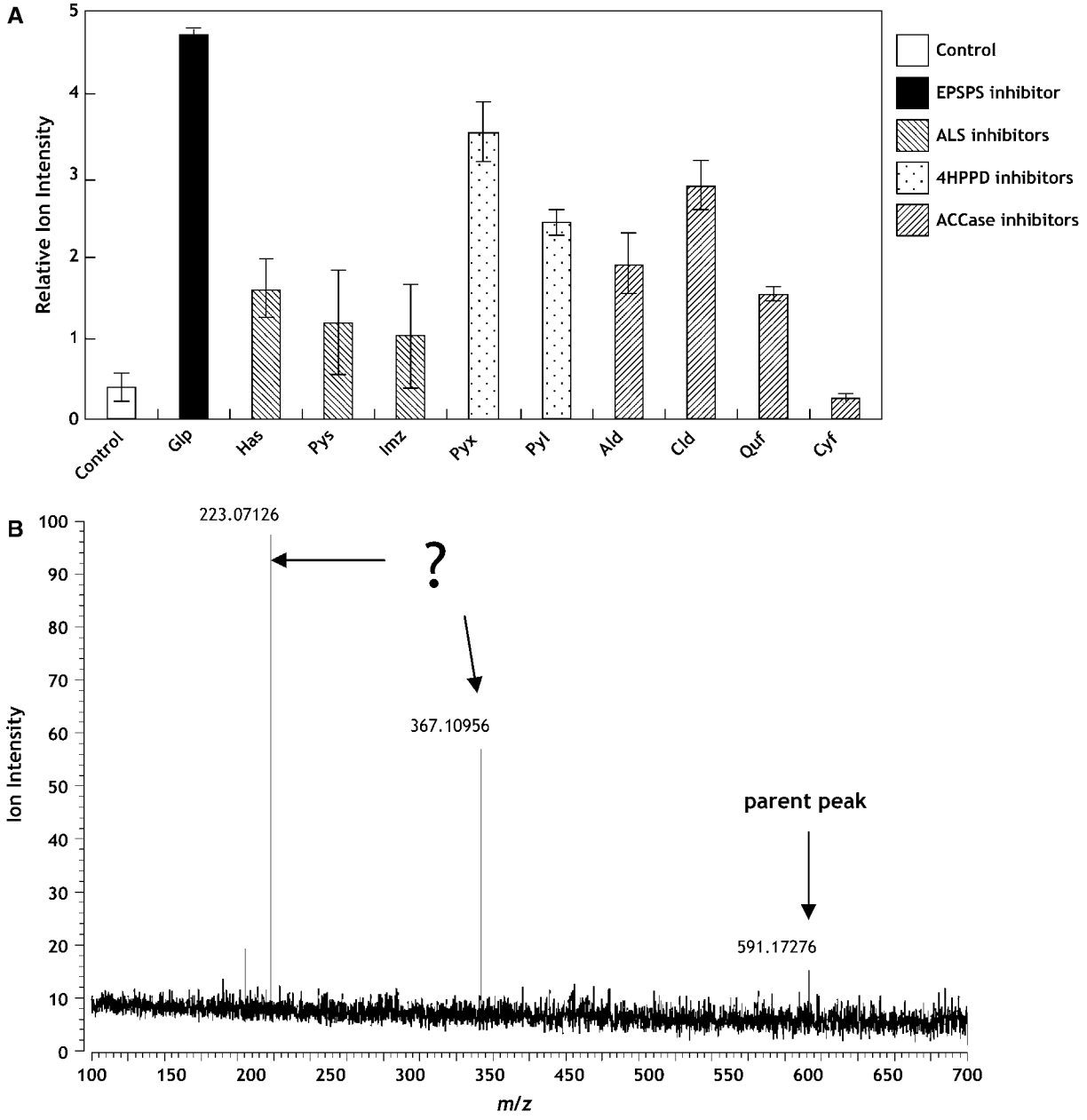

Figure 10. A, An ion (*m/z* = 591.17276) accumulated in Arabidopsis seedlings. Abbreviations for herbicides used for the metabolome analyses were shown in Table I. Error bars indicate SDs of three replicates. B, The KNApSAcK database search suggested a dirhamnosylflavonol ($C_{28}H_{32}O_{14}$) as the candidate for the ion with *m/z* = 591.17276. The MS/MS fragmentation pattern did not match the loss of Rha, and no corresponding candidate compounds were found in the KNApSAcK database.

observations suggested that the Arabidopsis ACCase enzymes could be resistant toward the herbicides, whereas Arabidopsis growth was strongly inhibited by the ACCase inhibitors quizalofop, alloxidim, and clethodim (Fig. 4). The Arabidopsis growth inhibition by the herbicides (Fig. 4) might implicate essential roles of multifunctional ACCase in Arabidopsis growth, whose functions could not be compensated by the multisubunit-type enzyme in chloroplasts. It has been suggested that quizalofop could inhibit ACC1 in Arabidopsis (Baud et al., 2004), leading to the depletion of cytosolic malonyl-CoA, which could not be transported from chloroplasts across the envelope. It has been reported that the herbicide-binding cooperativity correlated with the sensitivities of ACCase enzymes from grass species (Price et al., 2003), and herbicide sensitivities of Arabidopsis ACCase proteins should be clarified. It is also possible that the insensitivity toward cyhalofop may be due to different resistance mechanisms such as herbicide detoxification in Arabidopsis (Vila-Aiub et al., 2005).

Accumulation of Specific Metabolites by the Specific Enzyme Inhibition Treatments

In the ALS inhibitor treatments, specific accumulation of an ion with *m/z* = 577.15715 was observed in the negative ion mode (Fig. 8A). The KNApSAcK database search suggested a flavonol with two glycosides as a candidate for this ion. An MS/MS analysis was done with a parent peak (*m/z* = 577.15715), yielding two fragment peaks with *m/z* = 431.10115 and *m/z* = 285.04995, indicating the loss of one glycoside and two glycosides, respectively (Fig. 8B). Thus, dissociated ions could be a glycoside with the chemical formula of $C_6H_{12}O_5$, and the original ion with *m/z* = 577.15715 was suggested to be a trihydroxy flavonol ($C_{27}H_{30}O_{14}$). An ion with *m/z* = 531.18791 also accumulated in the ALS treatment (Fig. 9A). The KNApSAcK database search found a candidate, icaritin-3-rhamnoside [$C_{27}H_{32}O_{11}$; theoretical *m/z* = 531.18719 ($[M-H]^-$)]. The MS/MS analysis suggested the loss of the ion with the *m/z* value corresponding to one Rha moiety (Fig. 9B). While icaritin-3-rhamnoside is an unusual flavonoid derivative isolated only from *Epimedium sagittatum* (Mizuno et al., 1987), this metabolite has exactly the same chemical formula as icaritin-3-rhamnoside, and the MS/MS analysis was in good agreement with the presence of one sugar chain corresponding to Rha.

An ion with *m/z* = 591.17276 detected in the negative ion mode accumulated in plants treated with all herbicides except for cyhalofop (Fig. 10A), which had no growth inhibition activity for Arabidopsis (Figs. 4 and 5). A dirhamnosylflavonol ($C_{28}H_{32}O_{14}$) was suggested as the candidate for this ion through the KNApSAcK database search. However, the result of MS/MS analysis did not match the expected fragmentation patterns from a dirhamnosylflavonol (Fig. 10B). The *m/z* values of the two fragment ions did not correspond to the loss of Rha. While the structure of this metabolite was not elucidated, this compound could be a general marker metabolite for plant responses against herbicide treatment.

The KNApSAcK species-metabolite database has been constructed with published chemical structures with organism species information (Shinbo et al., 2006), and therefore, it is thought that the prediction of metabolite identities with species information could be fairly reliable. However, in the MS/MS analyses coupled with the KNApSAcK database search, we were not able to obtain direct information on stereochemical aspects, such as sugar conformation or hexose identity. Different analytical methods are essential to confirm chemical structures especially with multiple database hits of several stereoisomers. Incorporating chromatographic separation systems into the FT-ICR/MS system should be helpful in both reducing the ion suppression effects and comparing metabolites between different MS technologies and NMR studies.

Metabolic Phenotyping

Herbicides are expected to act on specific sites, while other physiological processes could be affected as well. For example, it has been reported that glyphosate, a specific EPSPS inhibitor, influenced carbon assimilation (Servaites et al., 1987). Comprehensive information for such side effects should be provided for the development of novel bioactive compounds, and metabolic profiling analyses could play a crucial role in uncovering hidden effects of chemical compounds on physiological processes. Aranìbar et al. (2001) have reported the classification and identification of herbicidal modes of action using ^{1}H-NMR coupled with an artificial neural network analysis. They achieved a rapid detection method to monitor the changes in total metabolic profiles, while information about individual metabolites contributing such metabolic fluctuations was to be provided by other analytical means.

Using the DMASS scheme (Supplemental Data S2), we were able to differentiate metabolic phenotypes representing specific pathway inhibitions caused by chemical compounds. The FT-ICR/MS-based metabolic phenotyping scheme consists of the DMASS for automatic mass-error correction and statistic analyses, the MS/MS structural analysis, and the KNApSAcK database incorporating more than 10,000 metabolite entries with literature references. This metabolomics tool specifically developed for FT-ICR/MS constitutes an important part of integrated metabolomics research platform.

MATERIALS AND METHODS

Chemicals

Glyphosate was purchased from Sigma-Aldrich, and quizalofop-ethyl was obtained from Dr. Ehrenstorfer. Pyrazolate was kindly supplied by Sankyo Agro. Other herbicides including pyrazosulfron-ethyl, halosulfuron-methyl, imazamox, pyrazoxyfen, alloxydim-sodium, chethodim, and cyhalofop-butyl

were purchased from Wako Pure Chemical Industries. Lidocaine and bombesin were purchased from Sigma-Aldrich, and tetra-*N*-acetylchitotetraose was from Seikagaku Kogyo. Other chemicals were purchased from Wako Pure Chemical Industries.

Plant Materials and Treatment with Herbicides

For germination, Arabidopsis (*Arabidopsis thaliana*) ecotype Columbia seeds were surface sterilized and placed on Suc-free germination medium (Valvekens et al., 1988) containing concentrations of herbicides. After a cold treatment for homogenous germination (two nights at 4°C), plants were grown at 20°C with continuous illumination for 1 week under a sterile condition.

Sample Preparation

Thirty 1-week-old plants were frozen in liquid N_2 and ground to powder, which was used for methanol extraction. The extracts were filtered through disposable membrane filter units (DISMIC-13JP, ADVANTEC), evaporated under N_2 atmosphere, and stored at −80°C until use. Upon FT-ICR/MS analysis, the extracts were dissolved in 50% (v/v) acetonitrile/water. IMCs for the positive ion mode were lidocaine ($[M + H]^+ = 235.18049$), prochloraz ($[M + H]^+ = 376.03809$), reserpine ($[M + H]^+ = 609.28066$), and bombesin ($[M + 2H]^{2+} = 810.41481$). A set of 2,4-dichlorophenoxy acetic acid ($[M-H]^- = 218.96212$), ampicillin ($[M-H]^- = 348.10235$), 3-[(3-cholamidopropyl) dimethylammonio] propanesulfonic acid ($[M-H]^- = 613.38920$), and tetra-*N*-acetylchitotetraose ($[M-H]^- = 829.32078$) were used as the IMCs in the negative ion mode analysis.

FT-ICR/MS Conditions

Mass analysis was done using an IonSpec Explorer FT-ICR/MS (IonSpec) equipped with a 7-tesla actively shielded superconducting magnet. Ions were generated from an ESI source with a fused silica needle of 0.005-inch i.d. Samples were infused using a Harvard syringe pump model 22 at a flow rate of 0.5 to 1.0 μL min^{-1} through a 100-μL Hamilton syringe. All the experimental events were controlled using Omega8 software (IonSpec). Briefly, the potentials on the electrospray emitters were set to 3.0 kV and −3.0 kV for the positive and the negative electrosprays, respectively. The base pressure in the source region was approximately 5×10^{-5} torr (1 torr = 133.3 Pa). For the positive and negative electrosprays, sample solutions were prepared in 50% (v/v) acetonitrile/water with 0.1% (v/v) of formic acid and ammonium hydroxide, respectively. Ionized metabolites were accumulated for a period of 2,500 to 5,000 ms in a hexapole ion trap/guide and transferred through a radiofrequency-only quadrupole into the FT-ICR cell in the superconducting magnetic field, where they were again trapped. The direct current potentials in the positive and negative ion mode analyses were −2 V and 2 V during the ion accumulation and 2 V and −2 V for the ion transfer into the FT-ICR cell, respectively. These ions trapped in the hexapole were extracted for the transfer into the FT-ICR cell. In the positive and negative ion modes, the potentials on the extraction plate were 12 V and −12 V during the ion trapping and were reversed to −2 V and 2 V for the extraction. The base pressure in the analyzer region was set to the level of approximately 4×10^{-10} torr. ESI-MS spectra were acquired over the *m/z* range 55 to 1,000 from 1,024,000 independent data points. MS/MS analyses were done using the sustained off-resonance irradiation SORI-CID methods (Gauthier et al., 1991; Laskin and Futrell, 2005). SORI R_f was set at 0.5 to 1.5 V, and the N_2 collision gas was used with 400-ms pulse.

Species-Metabolite Relationship Database

For systematic and comprehensive understanding of species-specific metabolic diversities, we have designed a database system, KNApSAcK, for searching relationships between metabolites and species (Shinbo et al., 2006). The database has incorporated a tool for analyzing datasets acquired by FT-ICR/MS. KNApSAcK consists of information about metabolite names, molecular formulas, structural formulas, species names, Chemical Abstract Service (CAS) registration numbers, and biological activities. All the KNApSAcK data were collected from published literature. Metabolites are checked for the accuracy of both molecular formulas and structural formulas using the CAS database, and the CAS registration numbers are obtained from the same database. Species names were checked for the accuracy of spelling using the National Center for Biotechnology Information Taxonomy Browser (http://www.ncbi.nlm.nih.gov/Taxonomy/), the Plants Database (http://plants.usda.gov/index.html), and the Integrated Taxonomic Information System (http://www.itis.usda.gov/). A total of 25,930 metabolite-species pairs encompassing 11,075 metabolites and 8,557 species were obtained from about 7,600 published references (January 19, 2006). These data have been stored on a server, which is located in the Nara Institute of Science and Technology. The database system is freely available at http://kanaya.naist.jp/KNApSAcK/ on the Java 1.4.2.

Supplemental Data

The following materials are available in the online version of this article.

Supplemental Data S1. FT-ICR/MS metabolomics data from the herbicide treatments.

Supplemental Data S2. DMASS instruction manual.

Received March 15, 2006; accepted August 4, 2006; published August 11, 2006.

LITERATURE CITED

Abe T, Kanaya S, Kinouchi M, Ichiba Y, Kozuki T, Ikemura T (2003) Informatics for unveiling hidden genome signatures. Genome Res **13:** 693–702

Aharoni A, Ric de Vos CH, Verhoeven HA, Maliepaard CA, Kruppa G, Bino R, Goodenowe DB (2002) Nontargeted metabolome analysis by use of Fourier transform ion cyclotron mass spectrometry. OMICS **6:** 217–234

Aranìbar N, Singh BK, Stockton GW, Ott KH (2001) Automated mode-of-action detection by metabolic profiling. Biochem Biophys Res Commun **286:** 150–155

Baud S, Bellec Y, Miquel M, Bellini C, Caboche M, Lepiniec L, Faure JD, Rochat C (2004) *gurke* and *pasticcino3* mutants affected in embryo development are impaired in acetyl-CoA carboxylase. EMBO Rep **5:** 515–520

Baud S, Guyon V, Kronenberger J, Wuillème S, Miquel M, Caboche M, Lepiniec L, Rochat C (2003) Multifunctional acetyl-CoA carboxylase 1 is essential for very long chain fatty acid elongation and embryo development in *Arabidopsis.* Plant J **33:** 75–86

Choi YH, Tapias EC, Kim HK, Lefeber AWM, Erkelens C, Verhoeven JTJ, Brzin J, Zel J, Verpoorte R (2004) Metabolic discrimination of *Catharanthus roseus* leaves infected by phytoplasma using ^{1}H-NMR spectroscopy and multivariate data analysis. Plant Physiol **135:** 2398–2410

Dehaye L, Alban C, Job C, Douce R, Job D (1994) Kinetics of the two forms of acetyl-CoA carboxylase from Pisum sativum. Correlation of the substrate specificity of the enzymes and sensitivity towards aryloxyphenoxypropionate herbicides. Eur J Biochem **225:** 1113–1123

Délye C, Zhang XQ, Chalopin C, Michel S, Powles SB (2003) An isoleucine residue within the carboxyl-transferase domain of multidomain acetyl-coenzyme A carboxylase is a major determinant of sensitivity to aryloxyphenoxypropionate but not to cyclohexanedione inhibitors. Plant Physiol **132:** 1716–1723

Délye C, Zhang XQ, Michel S, Matéjicek A, Powles SB (2005) Molecular bases for sensitivity to acetyl-coenzyme A carboxylase inhibitors in black-grass. Plant Physiol **137:** 794–806

Fernie AR, Trethewey RN, Krotzky AJ, Willmitzer L (2004) Metabolite profiling: from diagnostics to systems biology. Nat Rev Mol Cell Biol **5:** 763–769

Fiehn O (2002) Metabolomics: the link between genotypes and phenotypes. Plant Mol Biol **48:** 155–171

Fiehn O, Kopka J, Dörmann P, Altmann T, Trethewey RN, Willmitzer L (2000) Metabolite profiling for plant functional genomics. Nat Biotechnol **18:** 1157–1161

Gauthier JW, Trautman TR, Jacobson DB (1991) Sustained off-resonance irradiation for collision-activated dissociation involving Fourier transform mass spectrometry: collision-activated dissociation technique that emulates infrared multiphoton dissociation. Anal Chim Acta **246:** 211–225

Herbert D, Price LJ, Alban C, Dehaye L, Job D, Cole DJ, Pallett KE, Harwood JL (1996) Kinetic studies on two isoforms of acetyl-CoA carboxylase from maize leaves. Biochem J **318:** 997–1006

Hirai K, Uchida A, Ohno R (2002) Major synthetic routes for modern herbicide classes and agrochemical characteristics. *In* P Böger, K Wakabayashi, K Hirai, eds, Herbicide Classes in Development. Springer, Berlin, pp 179–289

Hirai MY, Kein M, Fujikawa Y, Yano M, Goodenowe D, Yamazaki Y, Kanaya S, Nakamura Y, Kitayama M, Suzuki H, et al (2005) Elucidation of gene-to gene and metabolite-to-gene networks in Arabidopsis by integration of metabolomics and transcriptomics. J Biol Chem **280:** 25590–25595

Hirai MY, Yano M, Goodenowe DB, Kanaya S, Kimura T, Awazuhara M, Arita M, Fujiwara T, Saito K (2004) Integration of transcriptomics and metabolomics for understanding of global responses to nutritional stresses in Arabidopsis thaliana. Proc Natl Acad Sci USA **101:** 10205–10210

Huhman DV, Sumner LW (2002) Metabolic profiling of saponins in *Medicago sativa* and *Medicago truncatula* using HPLC coupled to an electrospray ion-trap mass spectrometer. Phytochemistry **59:** 347–360

Huynh QK, Bauer SC, Bild GS, Kishore GM, Borgmeyer JR (1988) Site-directed mutagenesis of Petunia hybrida 5-enolpyruvylshikimate-3-phosphate synthase: Lys-23 is essential for substrate binding. J Biol Chem **263:** 11636–11639

Kanaya S, Kinouchi M, Abe T, Kudo Y, Yamada Y, Nishi T, Mori H, Ikemura T (2001) Analysis of codon usage diversity of bacterial genes with a self-organizing map (SOM): characterization of horizontally transferred genes with emphasis of the E. coli O157 genome. Gene **276:** 89–99

Kaplan F, Kopka J, Haskell DW, Zhao W, Schiller KC, Gatzke N, Sung DY, Guy CL (2004) Exploring the temperature-stress metabolome of Arabidopsis. Plant Physiol **136:** 4159–4168

Konishi T, Sasaki Y (1994) Compartmentalization of two forms of acetyl-CoA carboxylase in plants and the origin of their tolerance toward herbicides. Proc Natl Acad Sci USA **91:** 3598–3601

Kuk YI, Jung HI, Kwon OD, Lee do J, Burgos NR, Guh JO (2003) Sulfonylurea herbicide-resistant Monochoria vaginalis in Korean rice culture. Pest Manag Sci **59:** 949–961

Laskin J, Futrell JH (2005) Activation of large ions in FT-ICR mass spectrometry. Mass Spectrom Rev **24:** 135–167

Lichtenthaler HK (1990) Mode of action of herbicides affecting acetyl-CoA carboxylase and fatty acid biosynthesis. Z Naturforsch **45c:** 521–528

Mizuno M, Hanioka S, Suzuki N, Iinuma M, Tanaka T, Xin-shun L, Xhi-da M (1987) Flavonol glycosides from *Epimedium sagittatum.* Phytochemistry **26:** 861–863

Moss SR, Cocker KM, Brown AC, Hall L, Field LM (2003) Characterisation of target-site resistance to ACCase-inhibiting herbicides in the weed *Alopecurus myosuroides* (black-grass). Pest Manag Sci **59:** 190–201

Price LJ, Herbert D, Moss SR, Cole DJ, Harwood JL (2003) Graminicide insensitivity correlates with herbicide-binding co-operativity on acetyl-CoA carboxylase isoforms. Biochem J **375:** 415–423

Roessner U, Luedemann A, Brust D, Fiehn O, Linke T, Willmitzer L, Fernie AR (2001) Metabolic profiling allows comprehensive phenotyping of genetically or environmentally modified plant systems. Plant Cell **13:** 11–29

Ruiz-Santaella JP, Heredia A, Prado RD (2006) Basis of selectivity of cyhalofop-butyl in Oryza sativa L. Planta **223:** 191–199

Servaites JC, Tucci MA, Geiger DR (1987) Glyphosate effects on carbon assimilation, ribulose bisphosphate carboxylase activity, and metabolite levels in sugar beet leaves. Plant Physiol **85:** 370–374

Shinbo Y, Nakamura Y, Altaf-Ul-Amin M, Asahi H, Kurokawa K, Arita M, Saito K, Ohta D, Shibata D, Kanaya S (2006) KNApSAcK: a comprehensive species-metabolite relationship database. Biotechnol Agr Forest **57:** 166–181

Soga T, Ohashi Y, Ueno Y, Naraoka H, Tomita M, Nishioka T (2003) Quantitative metabolome analysis using capillary electrophoresis mass spectrometry. J Proteome Res **2:** 488–494

Steinrücken HC, Amrhein N (1980) The herbicide glyphosate is a potent inhibitor of 5-enolpyruvyl-shikimic acid-3-phosphate synthase. Biochem Biophys Res Commun **94:** 1207–1212

Sumner LW, Mendes P, Dixon RA (2003) Plant metabolomics: large-scale phytochemistry in the functional genomics era. Phytochemistry **62:** 817–836

Valvekens D, van Montagu M, van Lijsebettens M (1988) *Agrobacterium tumefaciens*-mediated transformation of *Arabidopsis thaliana* root explants by using kanamycin selection. Proc Natl Acad Sci USA **85:** 5536–5540

Viant MR, Rosenblum ES, Tjeerdema RS (2003) NMR-based metabolomics: a powerful approach for characterizing the effects of environmental stressors on organism health. Environ Sci Technol **37:** 4982–4989

Vila-Aiub MM, Neve P, Powles SB (2005) Resistance cost of a cytochrome P450 herbicide metabolism mechanism but not an ACCase target site mutation in a multiple resistant *Lolium rigidum* population. New Phytol **167:** 787–796

von Roepenack-Lahaye E, Degenkolb T, Zerjeski M, Franz M, Roth U, Wessjohann L, Schmidt J, Scheel D, Clemens S (2004) Profiling of Arabidopsis secondary metabolites by capillary liquid chromatography coupled to electrospray ionization quadrupole time-of-flight mass spectrometry. Plant Physiol **134:** 548–559

Widholm JM, Chinnala AR, Ryu JH, Song HS, Eggett T, Brotherton JE (2001) Glyphosate selection of gene amplification in suspension cultures of 3 plant species. Physiol Plant **112:** 540–545

Wu L, Mashego MR, van Dam JC, Proell AM, Vinke JL, Ras C, van Winden WA, van Gulik WM, Heijnen JJ (2005) Quantitative analysis of the microbial metabolome by isotope dilution mass spectrometry using uniformly ^{13}C-labeled cell extracts as internal standards. Anal Biochem **336:** 164–171

Zhang H, Tweel B, Tong L (2004) Molecular basis for the inhibition of the carboxyltransferase domain of acetyl-coenzyme-A carboxylase by haloxyfop and diclofop. Proc Natl Acad Sci USA **101:** 5910–5915